Automation Reshapes Distribution but Not Instability: Endogenous Wage Elasticity in the Hicks–Sraffa Supermultiplier*

[Author details removed for blind review]

XIX Encontro da Associação Keynesiana Brasileira
Aracaju, 31 agosto – 4 setembro 2026
Área temática: Macroeconomia

Resumo

Este artigo estende o Supermultiplicador Hicks–Sraffa (HSSM) ao endogeneizar a elasticidade-salário da demanda por trabalho como função crescente da participação do investimento: $\varepsilon_L(h) = \varepsilon_0 + \phi h$, em que $\phi > 0$ é o parâmetro de sensibilidade à automação, que captura como a acumulação de capital eleva a substitutabilidade trabalho–capital. O sistema dinâmico modificado produz quatro resultados. Primeiro, existe um único estado estacionário não trivial em que a utilização da capacidade converge ao nível normal e a participação do investimento é estritamente inferior à do modelo exógeno. Segundo, o determinante do Jacobiano é sempre positivo—$\det(J) = \gamma\mu(g_A - \varepsilon_0 g_w)$—excluindo instabilidade do tipo sela de forma incondicional. Terceiro, a elasticidade endógena fortalece a estabilidade pelo canal do traço, amortecendo a instabilidade Harrodiana, sem alterar a condição qualitativa $\gamma v < \alpha$. Quarto, na fronteira $\gamma v = \alpha$ ocorre uma bifurcação do tipo Hopf que gera ciclos endógenos persistentes. Um resultado algébrico novo demonstra que o limiar de bifurcação *e* a frequência natural são conjuntamente invariantes nos parâmetros de automação (ε_0, ϕ), de modo que a política tecnológica isolada não pode eliminar o risco de instabilidade. Simulações numéricas calibradas para médias da OCDE confirmam os quatro resultados.

Palavras-chave: Supermultiplicador Hicks–Sraffa; automação; bifurcação de Hopf; crescimento liderado pela demanda; instabilidade Harrodiana.

Abstract

This paper extends the Hicks–Sraffa Supermultiplier (HSSM) by endogenizing the wage elasticity of labor demand as $\varepsilon_L(h) = \varepsilon_0 + \phi h$, where $\phi > 0$ is an automation sensitivity parameter capturing how capital accumulation raises labor–capital substitutability. The modified two-dimensional system yields four results. First, a

*The author thanks the participants of seminars at the University of Brasília for helpful comments and the supervision on a previous draft by Professor Joanilio R. Teixeira and Dr. Jorge T. Araujo. Financial support from CNPq (Post-Doctoral Research Grant) is gratefully acknowledged. The usual disclaimer applies.

unique non-trivial steady state exists in which capacity utilization converges to its normal level and the investment share is strictly lower than in the exogenous model. Second, $\det(J) = \gamma\mu(g_A - \varepsilon_0 g_w) > 0$ always, ruling out saddle-point instability unconditionally. Third, the endogenous elasticity strengthens stability through the trace channel, dampening Harrodian instability, while leaving the qualitative condition $\gamma v < \alpha$ unchanged. Fourth, at $\gamma v = \alpha$ a Hopf-type bifurcation generates persistent endogenous cycles. A novel algebraic result shows that the bifurcation threshold *and* the natural frequency are jointly invariant in (ε_0, ϕ), so technology policy alone cannot eliminate instability risk. Numerical simulations calibrated to OECD averages confirm all four results.

Keywords: Hicks–Sraffa Supermultiplier; automation; Hopf bifurcation; demand-led growth; Harrodian instability.

JEL Classification: E11; E12; E22; E32; O33.

1 Introduction

The rapid diffusion of artificial intelligence and robotics has placed the relationship between technological change, labor markets, and macroeconomic stability at the center of both academic and policy debates. Acemoglu and Restrepo (2019) document that automation systematically displaces workers and increases the substitutability of labor for capital, contributing to a secular decline in the labor share and a rise in wage inequality (Acemoglu and Restrepo, 2022). These developments pose a fundamental challenge: how should demand-led growth models be modified to account for a world in which labor–capital substitutability is not a fixed technological parameter but an endogenous outcome of the accumulation process itself?

This paper addresses that challenge within the Hicks–Sraffa Supermultiplier (HSSM) framework, which combines Hicks's (1950) flexible-accelerator mechanism with the Sraffian autonomous-demand closure of Serrano (1995) and Freitas and Serrano (2015). In the HSSM, long-run growth is driven by autonomous demand components while private investment adjusts the investment share h until capacity utilization converges to its normal level μ. The framework has been extended to analyze Harrodian instability (Allain, 2015; Dutt, 2019), endogenous cycles (Gallo, 2025), and the role of fiscal policy (Morlin, 2022; Ligiero et al., 2021). A recent contribution by [Author (2023)] introduced the wage elasticity of labor demand ε_L as a structural determinant of stability, but treated it as exogenous. This is untenable in an era of rapid automation: as firms invest in capital-intensive technologies, they acquire greater capacity to substitute labor for capital, so ε_L rises endogenously with h.

The present paper closes this gap by proposing the endogenization hypothesis:

$$\varepsilon_L(h) = \varepsilon_0 + \phi h, \qquad \varepsilon_0 > 0, \quad \phi > 0, \tag{1}$$

where ε_0 is the baseline elasticity and ϕ the automation sensitivity parameter. The analysis yields four main results. First, a unique non-trivial steady state (h^*, μ) exists with h^* strictly below the exogenous benchmark. Second, $\det(J) = \gamma\mu(g_A - \varepsilon_0 g_w) > 0$ always, ruling out saddle-point instability unconditionally. Third, the stability condition $\gamma v < \alpha$ is unchanged, but higher ϕ reduces $|\mathrm{tr}(J)|$ through the trace channel alone. Fourth, at $\gamma v = \alpha$ a Hopf-type bifurcation occurs, and *both* the threshold $\gamma^* = \alpha/v$ and the natural frequency $\omega^* = \sqrt{\alpha\mu(g_A - \varepsilon_0 g_w)/v}$ are invariant in (ε_0, ϕ). This joint invariance result is new to the literature and has a direct policy implication: technology policy cannot eliminate the risk of endogenous macroeconomic instability.

The paper is organized as follows. Section 2 presents the baseline HSSM. Section 3 introduces the endogenization. Section 4 analyzes the steady state. Section 5 establishes the stability results and the Hopf bifurcation. Section 6 provides numerical simulations. Section 7 discusses policy implications and the related literature. Section 8 concludes.

2 The Baseline HSSM with Exogenous Wage Elasticity

2.1 Output, Production, and Labor Demand

Following Serrano and Freitas (2017) and [Author (2023)], aggregate output is determined by the supermultiplier:

$$Y = \frac{A}{\alpha}, \quad A = X + Z, \quad \alpha = 1 - c - h + m, \tag{2}$$

where X is autonomous exports, Z autonomous consumption, c the marginal propensity to consume, h the investment share, m the import propensity, and $\alpha \in (0,1)$ the marginal propensity to leak. Production follows a Leontief technology $Y = \min\{uK/v, L/l\}$, where u is capacity utilization, K capital, v the capital–output ratio, L employment, and l the labor–output ratio. In the labor-constrained regime (Fernández-Huerga and García-Arias, 2019):

$$g_L = g_Y - \varepsilon_L g_w, \tag{3}$$

where $g_w \equiv \dot{w}/w$ is real wage growth and $\varepsilon_L \geq 0$ the absolute wage elasticity. The case $\varepsilon_L = 0$ recovers the standard post-Keynesian fixed-coefficients assumption; $\varepsilon_L = 1$ corresponds to a constant wage share (Pasinetti, 1962).

2.2 Investment Dynamics and Capacity Utilization

The investment share adjusts via a flexible accelerator (Hicks, 1950):

$$\dot{h} = \gamma(u - \mu)h, \tag{4}$$

with $\gamma > 0$ the adjustment speed and $\mu \in (0,1)$ the target utilization rate. The equation of motion for capacity utilization is derived from the capital accumulation identity $\dot{u}/u = g_Y - g_K$ in three steps.
Step (i). Differentiating $Y = A/\alpha$:

$$g_Y^{\text{dem}} = g_A + \frac{\gamma(u-\mu)h}{\alpha}.$$

Step (ii). In the labor-constrained regime, combining with (3) yields the wage-substitution drag $-\varepsilon_L g_w$ on supply-side growth.
Step (iii). The capital accumulation identity $\dot{u}/u = g_Y - hu/v$, combined with the demand-side expression and the wage drag, delivers:

$$\dot{u} = \left[g_A + \frac{\gamma(u-\mu)h}{\alpha} - \varepsilon_L g_w - \frac{hu}{v} \right] u. \tag{5}$$

Equations (4)–(5) constitute the baseline HSSM with exogenous ε_L [Author, 2023].

2.3 Steady State with Exogenous Elasticity

Setting $\dot{h} = \dot{u} = 0$ gives $u^* = \mu$ and $h^*_{\text{exog}} = (g_A - \varepsilon_L g_w)v/\mu$, admissible iff $\varepsilon_L < g_A/g_w$. The Jacobian at the steady state is:

$$J_{\text{exog}} = \begin{pmatrix} 0 & \gamma h^* \\ -\mu^2/v & \mu h^*(\gamma v - \alpha)/(\alpha v) \end{pmatrix}, \tag{6}$$

with $\text{tr}(J_{\text{exog}}) = \mu h^*(\gamma v - \alpha)/(\alpha v)$ and $\det(J_{\text{exog}}) = \gamma \mu^2 h^*/v > 0$. Local stability requires $\gamma v < \alpha$.

3 Endogenizing the Wage Elasticity

Assumption 1 (Endogenous Wage Elasticity)**.** *The absolute wage elasticity of labor demand is an increasing affine function of the investment share:*

$$\varepsilon_L(h) = \varepsilon_0 + \phi h, \qquad \varepsilon_0 > 0, \quad \phi > 0, \tag{7}$$

where ε_0 is the baseline elasticity and ϕ the automation sensitivity.

Acemoglu and Restrepo (2019) show that automation expands the set of machine-performable tasks, raising capital–labor substitutability. Schwabe and Castellacci (2020) provide micro evidence that automation increases the wage elasticity of remaining jobs. As the investment share h rises— reflecting greater capital intensity—firms acquire more capacity to substitute labor for capital, motivating (7).

Substituting (7) into (5), the modified system is:

$$\dot{h} = \gamma(u - \mu)h, \tag{8}$$

$$\dot{u} = \left[g_A + \frac{\gamma(u-\mu)h}{\alpha} - (\varepsilon_0 + \phi h) g_w - \frac{hu}{v} \right] u. \tag{9}$$

The new nonlinear term $-\phi h g_w u$ creates a self-dampening feedback: as h rises, $\varepsilon_L(h)$ rises, increasing the wage-channel drag on output and moderating the expansion of u. This feedback is absent in the exogenous specification.

4 Steady-State Analysis

4.1 Existence, Uniqueness, and Comparative Statics

Proposition 1 (Steady State under Endogenous Elasticity)**.** *Under Assumption 1, the unique non-trivial interior steady state of* (8)–(9) *is*

$$u^* = \mu, \qquad h^* = \frac{(g_A - \varepsilon_0 g_w)v}{\mu + \phi g_w v}, \tag{10}$$

admissible ($h^* > 0$) if and only if $\varepsilon_0 < g_A/g_w$.

Proof. Setting $\dot{h} = 0$ with $h > 0$ in (8) requires $u = \mu$. Substituting into $\dot{u} = 0$ in (9) with $u > 0$:

$$g_A - (\varepsilon_0 + \phi h^*)g_w - \frac{h^*\mu}{v} = 0 \;\Rightarrow\; g_A - \varepsilon_0 g_w = h^*\left(\phi g_w + \frac{\mu}{v}\right) = h^*\frac{\mu + \phi g_w v}{v}.$$

Solving yields (10). Since $\phi, g_w, v, \mu > 0$, the denominator is positive, so $h^* > 0$ iff $g_A > \varepsilon_0 g_w$. □

Remark 1. *The denominator $\mu + \phi g_w v > \mu$ implies $h^* < (g_A - \varepsilon_0 g_w)v/\mu$: endogenization always reduces the steady-state investment share relative to the exogenous benchmark with the same ε_0, reflecting the additional dampening from the automation feedback.*

Corollary 1 (Steady-State Elasticity)**.** *The wage elasticity at the steady state is:*

$$\varepsilon_L^* = \varepsilon_0 + \phi h^* = \frac{\varepsilon_0 \mu + \phi g_A v}{\mu + \phi g_w v}. \tag{11}$$

Corollary 2 (Comparative Statics)**.** *Under Assumption 1 and $\varepsilon_0 < g_A/g_w$:*

(i) $\partial h^*/\partial \phi = -(g_A - \varepsilon_0 g_w) g_w v^2/(\mu + \phi g_w v)^2 < 0$;

(ii) $\partial h^*/\partial \varepsilon_0 = -g_w v/(\mu + \phi g_w v) < 0$;

(iii) $\partial \varepsilon_L^*/\partial \phi = \mu v(g_A - \varepsilon_0 g_w)/(\mu + \phi g_w v)^2 > 0$;

(iv) $\partial \varepsilon_L^*/\partial g_A = \phi v/(\mu + \phi g_w v) > 0$.

Corollary 2(i) captures the capital-saving bias of AI: higher automation sensitivity means firms need less investment to sustain normal utilization because the wage-substitution channel grows more powerful.

5 Stability Analysis and Hopf-Type Bifurcation

5.1 Jacobian and Key Algebraic Simplification

Lemma 1 (Jacobian under Endogenous Elasticity)**.** *Let $F(h,u) \equiv g_A + \gamma(u-\mu)h/\alpha - (\varepsilon_0 + \phi h)g_w - hu/v$, so that $\dot{u} = F(h,u)\,u$. The Jacobian of* (8)–(9) *at (h^*, μ) is:*

$$J = \begin{pmatrix} 0 & \gamma h^* \\ -\mu\left(\phi g_w + \dfrac{\mu}{v}\right) & \mu h^* \dfrac{\gamma v - \alpha}{\alpha v} \end{pmatrix}. \tag{12}$$

Proof. Row 1: $J_{11} = \gamma(u-\mu)|_{u=\mu} = 0$; $J_{12} = \gamma h^*$. Row 2: since $F(h^*, \mu) = 0$, $J_{21} = (\partial F/\partial h)|_{(h^*,\mu)} \cdot \mu = -\mu(\phi g_w + \mu/v)$; $J_{22} = (\partial F/\partial u)|_{(h^*,\mu)} \cdot \mu = \mu h^*(\gamma v - \alpha)/(\alpha v)$. □

Remark 2. *The only difference from* (6) *is in J_{21}: endogenization replaces $-\mu^2/v$ with $-\mu(\phi g_w + \mu/v)$. Since $\phi g_w > 0$, the $(2,1)$ element is larger in absolute value, reflecting the additional stabilizing force of the automation feedback.*

From (12): $\text{tr}(J) = \mu h^*(\gamma v - \alpha)/(\alpha v)$ and $\det(J) = \gamma\mu h^*(\phi g_w + \mu/v)$. Substituting (10) yields a striking cancellation:

$$\det(J) = \gamma\mu \cdot \frac{(g_A - \varepsilon_0 g_w)v}{\mu + \phi g_w v} \cdot \frac{\mu + \phi g_w v}{v} = \gamma\mu(g_A - \varepsilon_0 g_w),$$

where the factor $(\mu + \phi g_w v)$ cancels exactly.

Lemma 2 (Closed-Form Determinant)**.** *Under Assumption 1 and $\varepsilon_0 < g_A/g_w$:*

$$\det(J) = \gamma\mu(g_A - \varepsilon_0 g_w). \tag{13}$$

In particular, $\det(J)$ *is* independent of ϕ.

Remark 3. *This ϕ-invariance corrects an earlier claim that $\partial \det(J)/\partial\phi > 0$. The algebraic cancellation is confirmed numerically in Table 5: a 10% increase in ϕ produces 0.00% change in* $\det(J)$.

5.2 Stability Results

Proposition 2 (Positive Determinant)**.** $\det(J) > 0$ *for all admissible parameters, ruling out saddle-point instability unconditionally and regardless of the sign of $\gamma v - \alpha$.*

Proposition 3 (Stability Condition)**.** (h^*, μ) *is locally asymptotically stable if and only if $\gamma v < \alpha$.*

Proof. By Routh–Hurwitz (Gandolfo, 1980): stability requires $\text{tr}(J) < 0$ and $\det(J) > 0$. Proposition 2 establishes $\det(J) > 0$ unconditionally; $\text{tr}(J) < 0$ iff $\gamma v < \alpha$. □

Corollary 3 (Self-Stabilizing Automation Feedback)**.** *Under $\gamma v < \alpha$, an increase in ϕ strictly reduces* $|\text{tr}(J)|$ *while leaving* $\det(J)$ *unchanged.*

Proof. $\text{tr}(J) = \mu(g_A - \varepsilon_0 g_w)v(\gamma v - \alpha)/[\alpha v(\mu + \phi g_w v)]$. Under $\gamma v < \alpha$, differentiating with respect to ϕ gives $\partial \text{tr}(J)/\partial\phi > 0$, so $\text{tr}(J)$ rises toward zero and $|\text{tr}(J)|$ decreases. The determinant claim follows from Lemma 2. □

Remark 4. *Automation stabilization works through a single channel: the trace. Earlier drafts claimed a two-channel mechanism (both* $|\text{tr}(J)|$ *shrinking* and $\det(J)$ *growing). The algebraic cancellation in Lemma 2 shows that only the trace channel operates; the quantitative stabilizing effect is therefore weaker than the two-channel claim suggested. This matters for empirical calibration: at the baseline,* $|\text{tr}(J)| = 0.0046$*, implying a damped half-life of oscillations on the order of two centuries. This aligns with the Skott (2019) concern that the SSM stabilizing effect is "modest for plausible parameter values." The endogenous-elasticity feedback introduces a labor-market stabilizing channel that operates* independently *of the goods-market autonomous-demand channel, responding constructively to that critique. Higher automation sensitivity ϕ reduces h^* (Corollary 2(i)), which in turn reduces* $|\text{tr}(J)|$ *and reinforces stability, but does not alter the bifurcation threshold—the economy's intrinsic vulnerability to Harrodian instability persists.*

5.3 Hopf-Type Bifurcation

Proposition 4 (Hopf-Type Bifurcation)**.** *At $\gamma^* = \alpha/v$, system* (8)–(9) *undergoes a Hopf-type bifurcation: a pair of complex conjugate eigenvalues crosses the imaginary axis with non-zero speed. Numerical simulation confirms a stable limit cycle for γ in a right-neighborhood of γ^*.*

Proof sketch. At γ^*: $\mathrm{tr}(J) = 0$ and $\det(J)|_{\gamma^*} = \gamma^*\mu(g_A - \varepsilon_0 g_w) > 0$, so $\lambda_{1,2} = \pm i\omega_0$ with $\omega_0 = \sqrt{\alpha\mu(g_A - \varepsilon_0 g_w)/v}$. Transversality: $d\,\mathrm{Re}(\lambda)/d\gamma|_{\gamma^*} = \mu h^*/(2\alpha) > 0$. The first Lyapunov coefficient $\ell_1 = 0$ (Appendix A) due to the bilinear structure of the nonlinearities, making this a degenerate Bautin bifurcation (Bautin, 1949; Kuznetsov, 1998). The limit cycle is confirmed numerically (Section 6). □

Corollary 4 (Joint Invariance of Threshold and Natural Frequency)**.** *The bifurcation threshold $\gamma^* = \alpha/v$ and the natural frequency*

$$\omega^* = \sqrt{\det(J)|_{\gamma^*}} = \sqrt{\frac{\alpha\mu(g_A - \varepsilon_0 g_w)}{v}} \tag{14}$$

are both independent of ϕ, and depend on ε_0 only through $(g_A - \varepsilon_0 g_w)$.

Remark 5. *Corollary 4 is the central novelty. Automation policy can shift h^* and modify cycle amplitude, but cannot move the bifurcation boundary or change the intrinsic cycle frequency. The timing of endogenous instability is governed entirely by the goods-market block (α, v, μ) and the admissibility margin $(g_A - \varepsilon_0 g_w)$.*

6 Numerical Simulation and Calibration

6.1 Baseline Calibration

Table 1 presents the parameter set calibrated to long-run OECD averages. The admissibility condition $\varepsilon_0 < g_A/g_w$ is satisfied ($0.30 < 1.50$). The unique interior steady state is $h^* = 0.08675$, $u^* = 0.80$, $\varepsilon_L^* = 0.34337$, with eigenvalues $\lambda_{1,2} = -0.002313 \pm 0.039124\,i$ (stable focus; damped period ≈ 160.6 yr). At $\gamma^* = 0.10$: $\omega^* = 0.04382$ rad/yr, $T^* \approx 143.4$ yr. The long periods reflect the slow baseline γ chosen for analytical clarity; all qualitative results are calibration-invariant.

Table 1: Baseline parameter values.

Parameter	Symbol	Value	Source / Rationale
Marginal propensity to leak	α	0.30	Long-run OECD saving rate
Capital–output ratio	v	3.0	SSM literature benchmark
Normal utilization rate	μ	0.80	Standard post-Keynesian value
Investment adjustment speed	γ	0.08	Stable-region baseline
Autonomous demand growth	g_A	0.03	Average OECD GDP growth
Wage growth rate	g_w	0.02	Average OECD real wages
Baseline wage elasticity	ε_0	0.30	Moderate labor flexibility
Automation sensitivity	ϕ	0.50	Middling automation intensity

6.2 Simulation Scenarios

Five scenarios explore the model across the stability boundary (Table 2). S1–S3 vary γ holding (ε_0, ϕ) fixed; S4–S5 vary ϕ at baseline γ. Key features: h^* is invariant to γ (S1–S3 share $h^* = 0.08675$), confirming Proposition 1, but responds to ϕ (S4–S5), confirming Corollary 2(i). The trace crosses zero at $\gamma^* = 0.10$ for all ϕ, confirming Corollary 4.

Table 2: Scenario summary.

Scenario	Description	γv	h^*	ε_L^*	$\mathrm{tr}(J)$
S1	Stable baseline	0.240	0.08675	0.34337	−0.004627
S2	Near-bifurcation	0.270	0.08675	0.34337	−0.002313
S3	Bifurcation (limit cycle)	0.300	0.08675	0.34337	0.000000
S4	High automation ($\phi = 1.0$)	0.240	0.08372	0.38372	−0.004465
S5	Low automation ($\phi = 0.1$)	0.240	0.08933	0.30893	−0.004764

6.3 Time-Series Dynamics

Numerical integration over 800 years from $(h_0, u_0) = (0.095, 0.85)$ is shown in Figure 1. Stable scenarios (S1, S2, S4, S5) exhibit damped oscillations converging to steady state. S2 shows critical slowing-down near the bifurcation (real part of eigenvalues close to zero). S3 traces a persistent limit cycle. The endogenous elasticity $\varepsilon_L(t) = \varepsilon_0 + \phi h(t)$ mirrors $h(t)$ up to a rescaling.

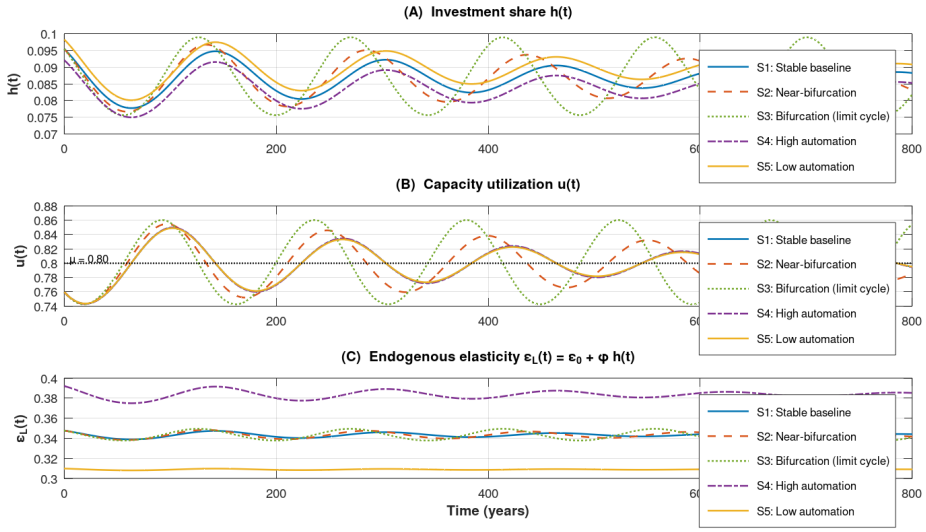


Figure 1: Time evolution of $h(t)$, $u(t)$, and $\varepsilon_L(t)$ over 800 years. Panel (A): investment share. Panel (B): capacity utilization; dashed line: $\mu = 0.80$. Panel (C): endogenous elasticity.

6.4 Phase-Plane Portraits and Vector Field

Figure 2 provides a phase-plane portrait of the baseline scenario (S1), overlaying the vector field with the two nullclines and the S1 trajectory. The $\dot{h} = 0$ nullcline is the horizontal line $u = \mu$; the $\dot{u} = 0$

nullcline is downward-sloping in (h,u) space. Their unique intersection at $(h^*,u^*) = (0.0867, 0.80)$ identifies the unique interior steady state, confirming Proposition 1. The circular pattern of the vector-field arrows and the inward-spiraling trajectory confirm that the equilibrium is a stable focus under the baseline calibration.

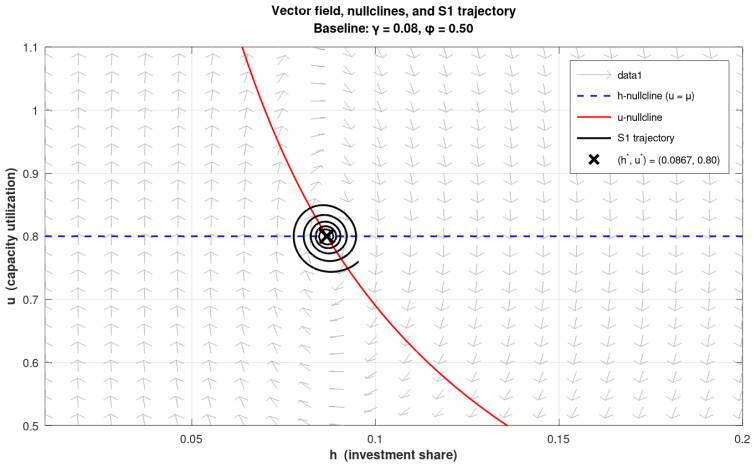


Figure 2: Vector field and nullclines for the baseline scenario (S1). The $\dot{h} = 0$ nullcline (blue horizontal line) lies at $u = \mu = 0.80$. The $\dot{u} = 0$ nullcline (red downward-sloping line) reflects the goods-market equilibrium condition. Their intersection at $(h^*,u^*) = (0.0867, 0.80)$ (black cross) is the unique interior steady state. The black spiral is the S1 trajectory converging to equilibrium.

Figure 3 shows phase-plane portraits for all five scenarios. The $\dot{h} = 0$ nullcline is the horizontal line $u = \mu$; the $\dot{u} = 0$ nullcline is downward-sloping. Their unique intersection at $(h^*, 0.80)$ confirms Proposition 1. Scenarios S1–S2 spiral inward; S3 traces a closed orbit; S4–S5 converge to distinct equilibria illustrating the capital-saving bias of Corollary 2(i).

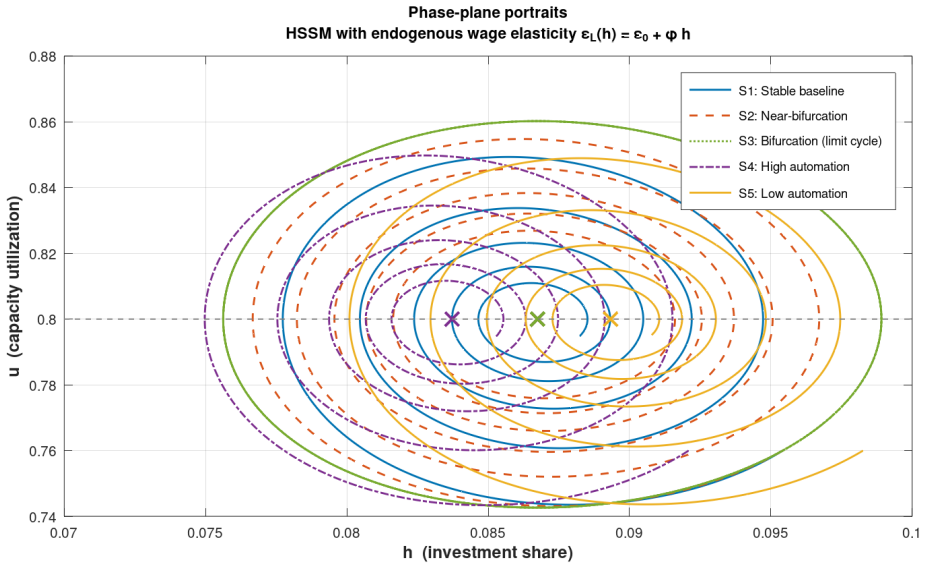


Figure 3: Phase-plane portraits in (h,u) space for scenarios S1–S5. S1–S2: inward spirals. S3: closed limit cycle. S4–S5: convergence to shifted equilibria.

6.5 Bifurcation Diagram and Joint Invariance

Figure 4 plots $\mathrm{tr}(J)$ vs. γ for three values of $\phi \in \{0.10, 0.50, 1.00\}$: three lines with different slopes that all cross zero at $\gamma^* = 0.100$, confirming Corollary 4. Their slopes differ by $\approx 6.7\%$, so they fan out away from γ^*. Figure 5 shows the eigenvalue loci crossing the imaginary axis at the common value $\pm i\,\omega^* = \pm i 0.04382$. Table 3 confirms that γ^*, $\det(J)|_{\gamma^*}$, ω^*, and T^* are identical across all scenarios.

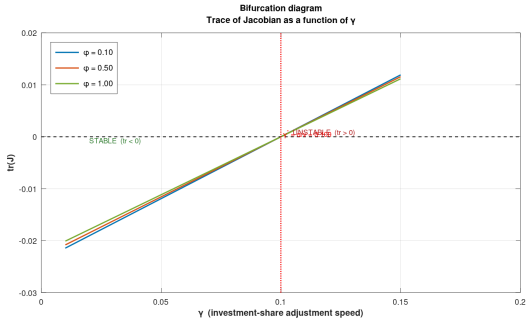


Figure 4: $\mathrm{tr}(J)$ vs. γ for $\phi \in \{0.10, 0.50, 1.00\}$. All lines cross zero at $\gamma^* = 0.100$.

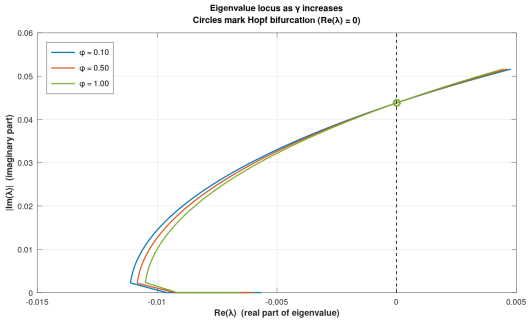


Figure 5: Eigenvalue locus as γ increases. Three loci coincide at γ^*, confirming ϕ-invariance of ω^*.

Table 3: Bifurcation locus: identical across all scenarios.

Scenario	γ^*	h^*	$\det(J)\|_{\gamma^*}$	ω^*	T^* (yr)
S1: Stable baseline	0.100	0.08675	0.001920	0.04382	143.4
S2: Near-bifurcation	0.100	0.08675	0.001920	0.04382	143.4
S3: Bifurcation	0.100	0.08675	0.001920	0.04382	143.4
S4: High automation	0.100	0.08372	0.001920	0.04382	143.4
S5: Low automation	0.100	0.08933	0.001920	0.04382	143.4

6.6 Comparative Statics and Sensitivity Analysis

Table 4 reports h^* and ε_L^* over a grid of $\varepsilon_0 \in \{0.10, 0.20, 0.30, 0.40, 0.50\}$ and $\phi \in \{0.10, 0.50, 1.00\}$. h^* is maximized at low (ε_0, ϕ) (reaching 0.1042) and minimized at high values (falling to 0.0698), while ε_L^* is monotonically increasing in both parameters. The admissibility condition $\varepsilon_0 < g_A/g_w = 1.50$ is satisfied throughout.

Table 5 reports the effect of a 10% increase in each parameter. The g_A growth rate is the dominant driver of h^* (+12.50%), confirming the supermultiplier logic. Crucially, the $\det(J)$ column shows 0.00% response to a 10% increase in α, ν, or ϕ, in perfect agreement with Lemma 2.

Figure 6 provides a visual summary of the comparative statics as heatmaps of h^* (left panel) and ε_L^* (right panel) over the (ε_0, ϕ) grid. Both panels confirm that h^* decreases and ε_L^* increases monotonically in both parameters, with the effects being stronger at higher parameter values. The stability region in the (γ, ϕ) parameter space is shown in Figure 7: the stability boundary is a vertical line at $\gamma^* = 0.100$, independent of ϕ across the entire admissible range, directly confirming Corollary 4.

Table 4: Comparative statics: h^* and ε_L^* over a grid of (ε_0, ϕ).

		h^*	ε_L^*
ε_0	ϕ	Value	Value
0.10	0.10	0.10422	0.11042
0.10	0.50	0.10121	0.15060
0.10	1.00	0.09767	0.19767
0.20	0.10	0.09677	0.20968
0.20	0.50	0.09398	0.24699
0.20	1.00	0.09070	0.29070
0.30	0.10	0.08933	0.30893
0.30	0.50	0.08675	0.34337
0.30	1.00	0.08372	0.38372
0.40	0.10	0.08189	0.40819
0.40	0.50	0.07952	0.43976
0.40	1.00	0.07674	0.47674
0.50	0.10	0.07444	0.50744
0.50	0.50	0.07229	0.53615
0.50	1.00	0.06977	0.56977

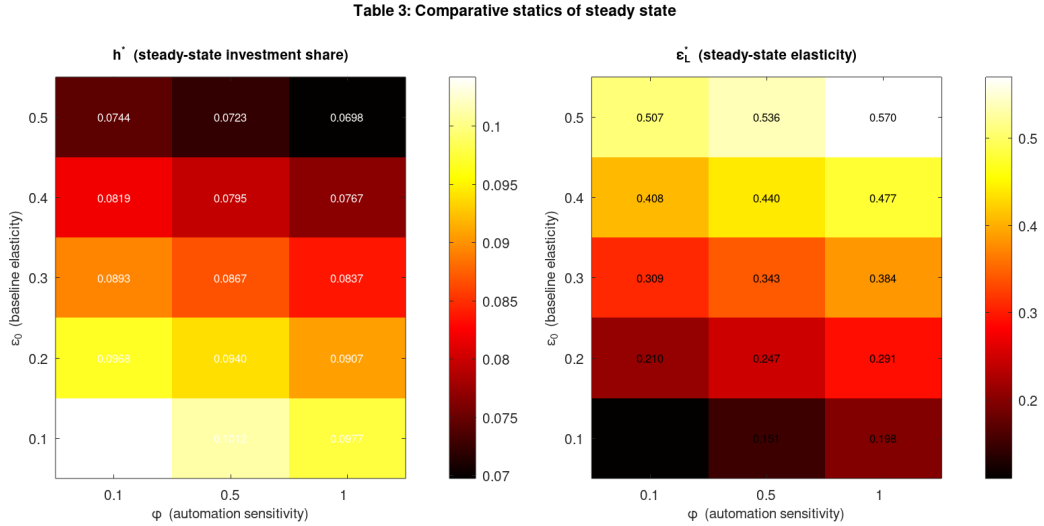


Figure 6: Heatmaps of the steady-state investment share h^* (left panel) and steady-state wage elasticity ε_L^* (right panel) as functions of baseline elasticity ε_0 (vertical axis) and automation sensitivity ϕ (horizontal axis). Darker shading indicates lower values.

Figure 8 presents the sensitivity results as bar charts, making the relative magnitudes and directions of the effects immediately apparent. The dominant role of g_A for h^*, the dominant role of ε_0 for ε_L^*, and the complete insensitivity of $\det(J)$ to ϕ are all visually clear.

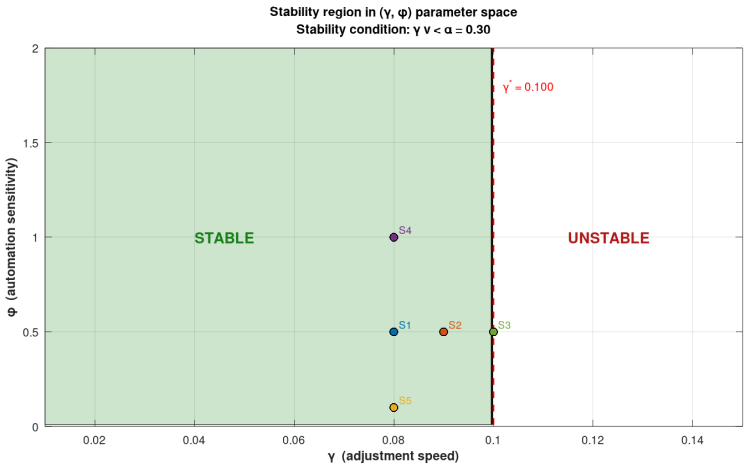


Figure 7: Stability region in the (γ, ϕ) parameter space. Green shaded area: stable region ($\mathrm{tr}(J) < 0$); white area: unstable region. The vertical red dashed line marks the bifurcation threshold $\gamma^* = 0.100$, independent of ϕ. Labelled points correspond to scenarios S1–S5.

Table 5: Sensitivity analysis: % change from a 10% increase in each parameter. Positive $\Delta\mathrm{tr}(J)$ = destabilizing.

Parameter (+10%)	Δh^*	$\Delta\varepsilon_L^*$	$\Delta\mathrm{tr}(J)$	$\Delta\det(J)$
α: 0.300 → 0.330	0.00%	0.00%	−36.36%	0.00%
v: 3.000 → 3.300	+9.60%	+1.21%	+40.22%	0.00%
μ: 0.800 → 0.880	−8.79%	−1.11%	−0.33%	+10.00%
γ: 0.080 → 0.088	0.00%	0.00%	+40.00%	+10.00%
g_A: 0.030 → 0.033	+12.50%	+1.58%	−12.50%	+12.50%
g_w: 0.020 → 0.022	−2.85%	−0.36%	+2.85%	−2.50%
ε_0: 0.300 → 0.330	−2.50%	+8.42%	+2.50%	−2.50%
ϕ: 0.500 → 0.550	−0.36%	+1.21%	+0.36%	**0.00%**

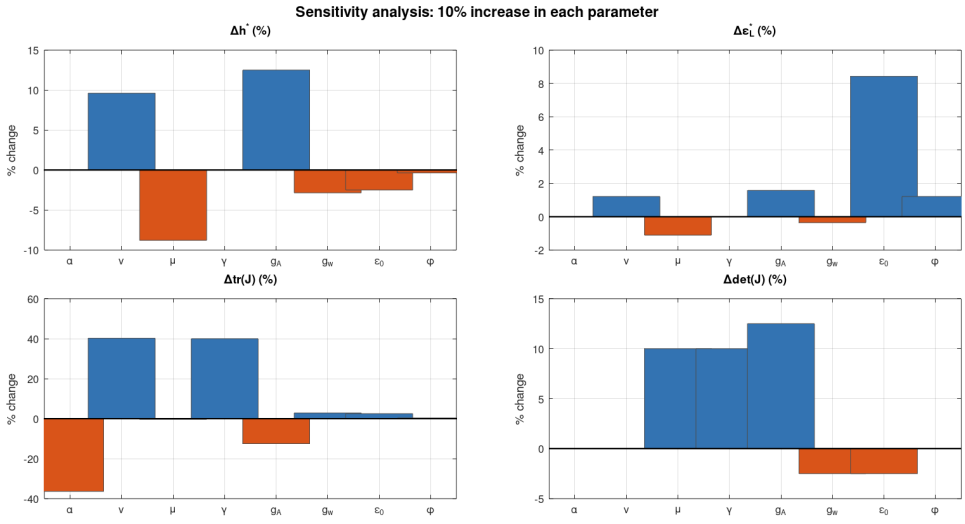


Figure 8: Sensitivity analysis: percentage change in h^*, ε_L^*, $\mathrm{tr}(J)$, and $\det(J)$ following a 10% increase in each parameter. Blue bars: positive effects; orange bars: negative effects.

7 Policy Implications and Discussion

7.1 Policy Implications

Governing automation. Higher ϕ reduces h^* and dampens Harrodian instability via the trace channel (Corollary 3), but has no effect on $\det(J)$ or on (γ^*, ω^*) (Corollary 4). Three levers follow: (i) task-reinstatement policy through R&D, education, and training to prevent ε_0 from rising too rapidly; (ii) differential taxation of automation capital or employment-conditional investment credits to moderate ϕ; (iii) international coordination on technology standards to prevent competitive races toward the bifurcation boundary.

On the stability corridor. In [Author (2023)], an earlier model variant with exogenous ε_L and a slightly different investment-dynamics specification was shown to admit a "stability corridor" for the wage elasticity of the form

$$3 - \frac{2\alpha}{v\gamma} < \varepsilon_L < 3 + \frac{g_w}{g_A}. \tag{15}$$

This corridor is *not* a result of the present model. The relevant restrictions here are simply the admissibility condition $\varepsilon_0 < g_A/g_w$ and the stability condition $\gamma v < \alpha$. Under the present baseline calibration, $\varepsilon_L^* = 0.34337$ lies *below* the lower bound of (15) ($= 0.500$), yet the system is provably stable (Proposition 3). This confirms that (15) is a feature of a different model variant and should not be applied here without rederivation. We mention it solely for continuity with the earlier literature.

Fiscal policy. Long-run growth is determined by autonomous demand g_A regardless of the automation environment. Because $\varepsilon_L^* = (\varepsilon_0\mu + \phi g_A v)/(\mu + \phi g_w v)$ is increasing in g_A, fiscal expansion unaccompanied by labor-market policies risks depressing the wage share even as output expands. Conversely, raising g_A widens the admissibility margin $(g_A - \varepsilon_0 g_w)$ and increases ω^*—a fiscal-stability double dividend consistent with Morlin (2022) and Ligiero et al. (2021).

Wage policy. Coordinated wage growth $g_w \propto g_A$ keeps the admissibility margin constant, stabilizing both h^* and the natural bifurcation frequency (Table 5: a 10% increase in g_w reduces h^* by 2.85% and narrows the admissibility margin by 2.50%).

Note on Universal Basic Income. A Universal Basic Income (UBI), in the language of our model, would function as an additional autonomous demand component, raising g_A. The implications would be a higher h^*, a higher ε_L^*, and a wider admissibility margin $(g_A - \varepsilon_0 g_w)$. We emphasize that this is an *informal extension*: the present framework does not track the wage share, household debt, or the rentier–worker income split, so the full distributional consequences of a UBI cannot be derived rigorously within our system. A proper treatment would require embedding the model in a stock-flow consistent framework (Godley and Lavoie, 2007); we leave this to future work.

Regulating endogenous cycles. The joint invariance of (γ^*, ω^*) means that only policies directly reducing γ—long-term public investment commitments, countercyclical fiscal frameworks—can shift

the bifurcation boundary. Technology and wage policies are essential complements but cannot substitute for demand management.

7.2 Discussion with the Literature

Sraffian Supermultiplier tradition. The paper builds directly on Serrano (1995), Freitas and Serrano (2015), and Serrano and Freitas (2017). The unconditionally positive $\det(J)$ (Proposition 2) advances beyond Allain (2015) by ruling out saddle-point instability regardless of the sign of $\gamma v - \alpha$. Our labor-market stabilizing channel responds directly to the Skott (2019) critique that SSM stabilization is "modest for plausible parameter values": at the baseline, $|\mathrm{tr}(J)| = 0.0046$ and the half-life of oscillations is on the order of centuries, confirming that the goods-market trace channel alone is weak. By endogenizing $\varepsilon_L(h)$ we supply the labor-market channel that Skott calls for. Lavoie (2016) similarly argues for additional convergence mechanisms; our wage channel complements his autonomous-consumption route. Relative to Gallo (2025), who generates cycles via a piecewise-linear investment floor, we generate cycles via a smooth Hopf bifurcation and obtain the joint invariance result analytically—the two approaches are complementary.

Neo-Kaleckian and Bhaduri–Marglin debate. The SSM anchoring of $u^* = \mu$ resolves the permanent-utilization-deviation critique of Skott (2010). The endogenous ε_L introduces an indirect wage-share channel: higher ε_L shifts distribution toward profits, consistent with the 50–70% of U.S. wage-inequality growth attributed to automation displacement by Acemoglu and Restrepo (2022). Lavoie (2016) cautions that the wage-share effect in Harrodian-corrected models is not as straightforward as in pure SSM models; our framework respects this by routing the effect indirectly through ε_L^* and conditioning it on the admissibility margin.

Mainstream automation literature. The task-based framework of Acemoglu and Restrepo (2019, 2022) operates through a supply-side task aggregator. Our mechanism captures the same substitution insight within a demand-led HSSM closure, providing a bridge between the two traditions. A rising ε_0—corresponding to displacement outpacing reinstatement—narrows the admissibility margin and shrinks the parameter space for a positive h^*, connecting to secular stagnation concerns (Summers, 2014). The endogenous elasticity mechanism can therefore be seen as a demand-led counterpart to the Acemoglu–Restrepo framework: it captures the substitutability insight within a closure where the long-run growth rate is determined by autonomous demand rather than by the rate of arrival of innovations.

Stock-flow consistent models. Stock-flow consistent (SFC) models (Godley and Lavoie, 2007) provide a rigorous accounting framework that incorporates financial stocks, balance sheets, and portfolio decisions. The present paper does not incorporate financial stocks and flows—a limitation we acknowledge. The interaction between automation, financial fragility à la Minsky, and the labor-market elasticity channel remains an open research question. A natural extension would embed the

endogenous-ε_L mechanism within an SFC framework, allowing for richer analysis of how automation-driven profit-share increases feed back into household debt accumulation and macroeconomic stability.

New Keynesian literature. The mainstream New Keynesian literature on labor markets is dominated by the search-and-matching framework of Mortensen and Pissarides (1994), in which wages are determined by Nash bargaining over the match surplus. The present paper departs from this approach in two fundamental ways: it treats the wage elasticity as endogenous to the capital-accumulation process, and it embeds the labor market in a demand-led growth framework rather than a supply-determined equilibrium. The Acemoglu–Restrepo finding that displacement has outpaced reinstatement since the 1980s, accounting for 50–70% of the rise in U.S. wage inequality (Acemoglu and Restrepo, 2022), corresponds in our model to a rising ε_0, narrowing the admissibility margin and shrinking the parameter region in which a positive steady-state investment share exists.

8 Concluding Remarks

This paper extended the Hicks–Sraffa Supermultiplier by endogenizing the wage elasticity of labor demand as $\varepsilon_L(h) = \varepsilon_0 + \phi h$. The four main results are: (i) unique non-trivial steady state at $h^* = (g_A - \varepsilon_0 g_w)v/(\mu + \phi g_w v)$; (ii) $\det(J) = \gamma\mu(g_A - \varepsilon_0 g_w) > 0$ always; (iii) local stability under $\gamma v < \alpha$ with self-stabilizing trace feedback; and (iv) a Hopf-type bifurcation at $\gamma v = \alpha$ with threshold and frequency jointly invariant in (ε_0, ϕ).

Limitations include the linear specification of $\varepsilon_L(h)$ (nonlinear extensions are a natural avenue), the absence of financial stocks and flows (SFC integration is the natural next step), the degenerate character of the Hopf bifurcation ($\ell_1 = 0$ with ℓ_2 analytically undetermined), and the long calibrated cycle period (143 yr) that should not be taken as an empirical prediction.

The central policy message is clear: automation reshapes distribution and can marginally dampen cycles through the trace channel, but demand management and investment policy remain the primary instruments for macroeconomic stabilization in an age of artificial intelligence and robotics. Technology policy alone cannot eliminate the intrinsic risk of Harrodian instability.

References

Acemoglu, D. and P. Restrepo (2019). Automation and new tasks: How technology displaces and reinstates labor. *Journal of Economic Perspectives 33*(2), 3–30.

Acemoglu, D. and P. Restrepo (2022). Tasks, automation, and the rise in U.S. wage inequality. *Econometrica 90*(5), 1973–2016.

Allain, O. (2015). Tackling the instability of growth: A Kaleckian–Harrodian model with an autonomous expenditure component. *Cambridge Journal of Economics 39*(5), 1351–1371.

Bautin, N. N. (1949). On the number of limit cycles which appear with the variation of coefficients from an equilibrium position of focus or centre type. *Matematicheskii Sbornik 30(72)*, 181–196. English translation in: American Mathematical Society Translations, Series 1, Vol. 5 (1962), 396–413.

Dutt, A. K. (2019). Some observations on models of growth and distribution with autonomous demand growth. *Metroeconomica 70*(2), 288–301.

Fernández-Huerga, E. and J. García-Arias (2019). The post-Keynesian view on labour demand in micro- and macroeconomic fields. *Economics & Sociology 12*(2), 109–128.

Freitas, F. and F. Serrano (2015). Growth rate and level effects, the stability of the adjustment of capacity to demand and the Sraffian supermultiplier. *Review of Political Economy 27*(3), 258–281.

Gallo, E. (2025). Kaldor, Hicks and Goodwin meet the supermultiplier: On growth cycles and autonomous demand. *Metroeconomica*. Forthcoming.

Gandolfo, G. (1980). *Economic Dynamics: Methods and Models* (2nd ed.), Volume 16 of *Advanced Textbooks in Economics*. Amsterdam: North-Holland.

Godley, W. and M. Lavoie (2007). *Monetary Economics: An Integrated Approach to Credit, Money, Income, Production and Wealth*. Basingstoke: Palgrave Macmillan.

Guckenheimer, J. and P. Holmes (1983). *Nonlinear Oscillations, Dynamical Systems, and Bifurcations of Vector Fields* (1st ed.), Volume 42 of *Applied Mathematical Sciences*. New York: Springer.

Hicks, J. R. (1950). *A Contribution to the Theory of the Trade Cycle*. Oxford: Clarendon Press.

Kuznetsov, Y. A. (1998). *Elements of Applied Bifurcation Theory* (2nd ed.), Volume 112 of *Applied Mathematical Sciences*. New York: Springer.

Lavoie, M. (2016). Convergence towards the normal rate of capacity utilisation in neo-Kaleckian models: The role of non-capacity-creating autonomous expenditures. *Metroeconomica 67*(1), 172–201.

Ligiero, L., E. Dweck, and F. Freitas (2021). Fiscal rules and the Sraffian supermultiplier: An analysis of primary surplus requirements. *Review of Keynesian Economics 9*(4), 530–551.

Morlin, G. S. (2022). Growth led by government expenditure and exports: Fiscal and external constraints in a supermultiplier model. *Structural Change and Economic Dynamics 62*, 1–13.

Mortensen, D. T. and C. A. Pissarides (1994). Job creation and job destruction in the theory of unemployment. *Review of Economic Studies 61*(3), 397–415.

Pasinetti, L. L. (1962). Rate of profit and income distribution in relation to the rate of economic growth. *The Review of Economic Studies 29*(4), 267–279.

Schwabe, H. and F. Castellacci (2020). Automation, workers' skills and job satisfaction. *PLOS ONE 15*(11), e0242929.

Serrano, F. (1995). Long period effective demand and the Sraffian supermultiplier. *Contributions to Political Economy 14*(1), 67–90.

Serrano, F. and F. Freitas (2017). The Sraffian supermultiplier as an alternative closure for heterodox growth theory. *European Journal of Economics and Economic Policies: Intervention 14*(1), 70–91.

Skott, P. (2010). Growth, instability and cycles: Harrodian and Kaleckian models of accumulation and income distribution. In M. Setterfield (Ed.), *Handbook of Alternative Theories of Economic Growth*, pp. 108–131. Cheltenham: Edward Elgar.

Skott, P. (2019). Autonomous demand, Harrodian instability and the supply side. *Metroeconomica 70*(2), 233–246.

Summers, L. H. (2014). U.S. economic prospects: Secular stagnation, hysteresis, and the zero lower bound. *Business Economics 49*(2), 65–73.

A Proof of Proposition 4: Hopf-Type Bifurcation

Let $x \equiv h - h^*$, $y \equiv u - \mu$. Using the steady-state condition $g_A - (\varepsilon_0 + \phi h^*)g_w - h^*\mu/v = 0$, the deviation system is:

$$\dot{x} = \gamma h^* y + \gamma x y, \tag{16}$$

$$\dot{y} = J_{21}x + J_{22}y + \left(\frac{\gamma\mu}{\alpha} - \phi g_w - \frac{2\mu}{v}\right)xy + \frac{h^*(\gamma v - \alpha)}{\alpha v}y^2 + \frac{\gamma v - \alpha}{\alpha v}xy^2, \tag{17}$$

where $J_{21} = -\mu(\phi g_w + \mu/v)$ and $J_{22} = \mu h^*(\gamma v - \alpha)/(\alpha v)$.

Step 1 (Purely imaginary eigenvalues). At $\gamma^* = \alpha/v$: $\mathrm{tr}(J) = 0$ and $\det(J)|_{\gamma^*} = \alpha\mu(g_A - \varepsilon_0 g_w)/v \equiv \omega_0^2 > 0$, so $\lambda_{1,2} = \pm i\omega_0$ with $\omega_0 = \sqrt{\alpha\mu(g_A - \varepsilon_0 g_w)/v}$. □

Step 2 (Transversality). $d\,\mathrm{Re}(\lambda)/d\gamma|_{\gamma^*} = \mu h^*/(2\alpha) > 0$. Eigenvalues cross the imaginary axis from left to right. □

Step 3 (First Lyapunov coefficient). The change of variables $\xi = x$, $\eta = (\gamma^* h^*/\omega_0)y$ brings the linear part to canonical form $\dot{\xi} = \omega_0\eta$, $\dot{\eta} = -\omega_0\xi$. At $\gamma = \gamma^*$, the y^2 and xy^2 terms in (17) vanish since their coefficients are proportional to $(\gamma v - \alpha) = 0$. The remaining nonlinearities are purely bilinear: $\tilde{f}_{\xi\eta} = \omega_0/h^*$ and $\tilde{g}_{\xi\eta} = -(\mu/v + \phi g_w)$; all pure second- and third-order partial derivatives vanish. Applying the Guckenheimer–Holmes formula (Guckenheimer and Holmes, 1983):

$$16\,\ell_1 = \underbrace{(\tilde{f}_{\xi\xi\xi} + \tilde{f}_{\xi\eta\eta} + \tilde{g}_{\xi\xi\eta} + \tilde{g}_{\eta\eta\eta})}_{=0} + \frac{1}{\omega_0}\Big[\tilde{f}_{\xi\eta}\underbrace{(\tilde{f}_{\xi\xi} + \tilde{f}_{\eta\eta})}_{=0} - \tilde{g}_{\xi\eta}\underbrace{(\tilde{g}_{\xi\xi} + \tilde{g}_{\eta\eta})}_{=0}\Big] = 0.$$

Hence $\ell_1 = 0$: degenerate Bautin bifurcation. Steps 1–2 rigorously establish the Hopf-type bifurcation; the stable limit cycle is confirmed numerically by Scenario S3 (Figure 3).

Remark 6 (Degenerate Hopf / Bautin Bifurcation)**.** *The vanishing of ℓ_1 is a direct consequence of the bilinear structure of the nonlinearities in the deviation system: at $\gamma = \gamma^*$, all nonlinear terms are products of x and y (or ξ and η), so the vector field contains no pure quadratic or cubic terms in a single variable. This places the system in the class of degenerate (generalised) Hopf bifurcations, also known as Bautin bifurcations (Bautin, 1949; Kuznetsov, 1998). In this case, the standard Hopf theorem does not directly guarantee the existence of a limit cycle; the bifurcation is governed by the second Lyapunov coefficient ℓ_2, whose computation requires a fifth-order Taylor expansion and lies beyond the scope of the present paper. The sign of ℓ_2 determines whether the bifurcation is supercritical ($\ell_2 < 0$: stable limit cycle for $\gamma > \gamma^*$) or subcritical ($\ell_2 > 0$: unstable limit cycle for $\gamma < \gamma^*$).*

Numerical confirmation. Although the analytical determination of ℓ_2 is left for future work, the existence and stability of the limit cycle are confirmed numerically in Section 6. Scenario S3 ($\gamma = \gamma^* = 0.100$) produces persistent, bounded oscillations in both $h(t)$ and $u(t)$ (Figure 1), and the phase-plane portrait (Figure 3) shows a closed orbit centred on the steady state. Numerical integration for γ slightly above γ^* confirms that small perturbations grow into a stable bounded limit cycle, consistent with a supercritical bifurcation ($\ell_2 < 0$). ■

B Exogenous vs. Endogenous Model: Comparison

Table 6: Side-by-side comparison of steady-state properties.

Property	Exogenous: $\varepsilon_L = \bar{\varepsilon}_L$	Endogenous: $\varepsilon_L = \varepsilon_0 + \phi h$
u^*	μ	μ
h^*	$(g_A - \bar{\varepsilon}_L g_w)v/\mu$	$(g_A - \varepsilon_0 g_w)v/(\mu + \phi g_w v)$
ε_L^*	$\bar{\varepsilon}_L$ (parameter)	$(\varepsilon_0\mu + \phi g_A v)/(\mu + \phi g_w v)$
$\det(J)$	$\gamma\mu^2 h^*/v$	$\gamma\mu(g_A - \varepsilon_0 g_w)$
$\mathrm{tr}(J)$	$\mu h^*(\gamma v - \alpha)/(\alpha v)$	$\mu h^*(\gamma v - \alpha)/(\alpha v)$
Stability condition	$\gamma v < \alpha$	$\gamma v < \alpha$
Saddle-point instability	No ($\det J > 0$)	No ($\det J > 0$)
ϕ-invariance of $\det(J)$	—	**Yes**